2020 IEEE International Conference on Robotics and Automation (ICRA)
31 May - 31 August, 2020. Paris, France

Distributed Consensus Control of Multiple UAVs in a Constrained Environment

Gang Wang, Weixin Yang, Na Zhao, Yunfeng Ji, Yantao Shen, Hao Xu, and Peng Li

Abstract— **In this paper, we investigate the consensus problem of multiple unmanned aerial vehicles (UAVs) in the presence of environmental constraints under a general communication topology containing a directed spanning tree. First, based on a position transformation function, we propose a novel dynamic reference position and yaw angle for each UAV to cope with both the asymmetric topology and the constraints. Then, the backstepping-like design methodology is presented to derive a local tracking controller for each UAV such that its position and yaw angle can converge to the reference ones. The proposed protocol is distributed in the sense that, the input update of each UAV dynamically relies only on local state information from its neighborhood set and the constraints, and it does not require any additional centralized information. It is demonstrated that under the proposed protocol, all UAVs reach consensus without violation of the environmental constraints. Finally, simulation and experimental results are provided to demonstrate the performance of the protocol.**

I. Introduction

Autonomous unmanned aerial vehicles (UAVs) are emerging as a disruptive technology to enable highly intelligent systems with significant influence on various fields of science, technology, and engineering, including surveillance, transportation, and mapping [1]. Coordination of multiple UAVs has been demonstrated to be more efficient than a single one, and allows the group to perform complex tasks that the individual cannot complete on its own; for instance, cooperative transportation [2] and cooperative aerial mapping [3] were reported. As a primary problem of coordination, distributed control of multiple UAVs that can ensure a collective behavior based on local interaction has been widely studied. Such a policy can simplify the configuration and implementation as well as enhance the robustness of the entire system while reducing communication costs. Through the use of the graph theory and the Lyapunov method, some distributed control strategies have been presented for multiple UAVs in the literature [4], [5]. One common restriction of these works mentioned above is to disregard the constraints of the environment that should be inevitably encountered in practical applications. In numerous scenarios, UAVs do maneuver in the environment, of which the operating ranges are quite limited, such as the indoor environment and dense forests.

Path planning takes an essential role in facilitating autonomous, aggressive, high-speed UAV flight through complex constrained environments. Within the framework of path planning, some research efforts have appeared to obtain optimal and feasible trajectories for UAVs in constrained and cluttered environments (see [6], [7], [8], [9] and the references therein). Nevertheless, these works centering on individual UAVs cannot be directly applied to handle the coordination issue of multiple UAVs. In [10], a trajectory generation algorithm for labeled multi-robot systems was proposed. However, such an algorithm is centralized and depends on a single base station, and it cannot be calculated and executed by each UAV in a distributed fashion, i.e., employing only locally available information. From a control perspective, the environmental constraints can be treated as the state (position) limitations of the considered system [11]. Recently, an adaptive consensus algorithm for a class of first-order multi-agent systems with state constraints has been provided in [12]. This result was generalized to higher-order output-constrained multi-agent systems in [13]. It is noted that these aforementioned results, relying heavily on the symmetric positive semi-definiteness of the Laplacian matrices on undirected graphs, cannot be implemented to the cases where the communication topologies are directed.

This work builds on these observations and considers the distributed control problem of multiple UAVs with general directed communication topologies in constrained environments. Specifically, the communication topology is assumed to contain a directed spanning tree. Utilizing a position transformation function, a new dynamic reference position and yaw angle are first developed for each UAV to deal with the environmental constraints and the directed communication topology. Then, the backstepping-like design methodology is used to derive a local tracking algorithm such that the position and yaw angle of each UAV can track the reference ones. It is shown that under the proposed protocol, all UAVs can realize consensus and their positions do not violate the environmental constraints. We clarify that our contributions are nontrivial in two significant aspects. First, contrary to the existing distributed control schemes on multiple UAVs [4], [5], this work focuses on the consensus problem in the presence of environmental constraints. To the best of our knowledge, it is the first time in the distributed control field of multiple UAVs. Second, unlike the output-constrained consensus methods under undirected communication topologies [12], [13], the proposed new control

G. Wang and Y. Ji are with the Institute of Machine Intelligence, University of Shanghai for Science and Technology, Shanghai 200093, China, and their work was supported by the Shanghai Artificial Intelligence Innovation and Development Special Support Project. G. Wang was with the Department of Electrical & Biomedical Engineering, University of Nevada, Reno, NV 89557, USA.

W. Yang, N. Zhao, Y. Shen, and H. Xu are with the Department of Electrical & Biomedical Engineering, University of Nevada, Reno, NV 89557, USA ytshen@unr.edu.

P. Li is with HIT Shenzhen, China, and his work was partially supported by JCYJ20180507183456108.

algorithm is capable of addressing the consensus problem and output constraints under a general directed graph. Moreover, since the UAV involves some particular characteristics such as the strong coupling nonlinearity, underactuation, and multi-variable nature, existing methods cannot be extended straightforwardly to the control of multiple UAVs.

II. Problem statement and preliminaries

A. Graph theory

A weighted directed graph $\mathcal{G} = (\mathcal{V}, \mathcal{E})$ with the node set $\mathcal{V} = \{1, \ldots, n\}$ and the edge set $\mathcal{E} \subseteq \mathcal{V} \times \mathcal{V}$ is adopted to describe the communication topology among the n UAVs. An edge $(i, j) \in \mathcal{E}$ indicates that node j can receive information from node i, and node i is a neighbor of node j. The set of all neighbors of node i is denoted by $\mathcal{N}_i$. A directed path from node i_1 to node i_p is a sequence of ordered edges in the form of (i_m, i_{m+1}), $m = 1, \ldots, p-1$. A directed graph is said to contain a directed spanning tree if there exists at least a node such that the node has directed paths to all other nodes in $\mathcal{G}$. The weighted adjacency matrix $\mathcal{A} = [a_{ij}] \in R^{n\times n}$ associated with $\mathcal{G}$ is defined by $a_{ij} > 0$ if $(j, i) \in \mathcal{E}$ and $a_{ij} = 0$ otherwise. The Laplacian matrix $\mathcal{L} = [l_{ij}] \in R^{n\times n}$ associated with $\mathcal{G}$ is defined as $l_{ii} = \sum_{j\in\mathcal{N}_i} a_{ij}$ and $l_{ij} = -a_{ij}, i \neq j$.

B. Problem statement

Let $\mathcal{B} = \{B_x B_y B_z\}$ represent the body fixed frame and its origin coincide with the mass center of the UAV. Let $p_i = [x_i, y_i, z_i]^T \in R^3$ be the position of the mass center of the ith UAV expressed in the fixed inertial frame, where $x_i \in R$, $y_i \in R$, and $z_i \in R$ are, respectively, the longitudinal, latitudinal, and vertical positions. $\gamma_i = [\phi_i, \theta_i, \psi_i]^T \in R^3$ denotes the attitude of the ith UAV, where $\phi_i \in R$ is the roll angle around the B_x axis, $\theta_i \in R$ is the pitch angle around the B_y axis, and $\psi_i \in R$ is the yaw angle around the B_z axis. The dynamic model of the ith UAV can be expressed as follows

$$\begin{aligned} \ddot{p}_i &= \tfrac{1}{m_i}\bar{R}_i T_i - \mathrm{g}\bar{e}_3, \\ \ddot{\gamma}_i &= f_i + g_i \tau_i, \end{aligned} \tag{1}$$

where $\bar{e}_3 = [0, 0, 1]^T$, $T_i \in R$ is the thrust on the body, $\tau_i \in R^3$ is the total moment for rotational motion, m_i denotes the mass of the ith UAV, g is the standard gravitational acceleration, $I_{i,x}, I_{i,y}, I_{i,z} \in R^+$ are the moment of inertia, $g_i = \mathrm{diag}\{1/I_{i,x}, 1/I_{i,y}, 1/I_{i,z}\}$, $f_i = [\frac{I_{i,y}-I_{i,z}}{I_{i,x}}\dot{\theta}_i\dot{\psi}_i, \frac{I_{i,z}-I_{i,x}}{I_{i,y}}\dot{\phi}_i\dot{\psi}_i, \frac{I_{i,x}-I_{i,y}}{I_{i,z}}\dot{\theta}_i\dot{\phi}_i]$, and

$$\bar{R}_i = \begin{bmatrix} \cos\phi_i \sin\theta_i \cos\psi_i + \sin\phi_i \sin\psi_i \\ \cos\phi_i \sin\theta_i \sin\psi_i - \sin\phi_i \cos\psi_i \\ \cos\phi_i \cos\theta_i \end{bmatrix}.$$

The main purpose of this work is to design a distributed control algorithm under a directed communication topology such that (i) all UAVs reach consensus by dynamically employing only local state information and the constraints, i.e., $\lim_{t\to\infty}[(p_i(t) - \triangle_i(t)) - (p_j(t) - \triangle_j(t))] = \mathbf{0}_3$[1] and $\lim_{t\to\infty}(\psi_i(t) - \psi_j(t)) = 0$, and (ii) the position of each UAV lies in a pre-defined range during the operation, i.e., $L_\nu < \nu_i(t) - \triangle_i(t) < U_\nu$, $\forall t \geq 0$, where $\nu = x, y, z$, $\triangle_i(t) = [\triangle_{i,x}(t), \triangle_{i,y}(t), \triangle_{i,z}(t)]^T \in R^3$ denotes the time-varying offset of the desired distance between the ith UAV and the consensus position, and $L_\nu \in R$ and $U_\nu \in R$ satisfying $L_\nu < U_\nu$ represent the constant constraints of the environment.

Assumption 1: The initial positions of all UAVs satisfy the environmental constraints, i.e., $L_\nu < \nu_i(0) - \triangle_{i,\nu}(0) < U_\nu$ for all $\nu = x, y, z$.

III. Control protocol design

In this section, control protocol design is presented for the multiple UAVs (1) in a constrained environment. Similar to [14], we develop a novel position transformed function incorporating environmental constraints for the ith, $i = 1, \ldots, n$, UAV as $\bar{p}_i = [\bar{x}_i, \bar{y}_i, \bar{z}_i]^T$, where

$$\bar{\nu}_i = \ln((\nu_i - \triangle_{i,\nu}) - L_\nu) - \ln(U_\nu - (\nu_i - \triangle_{i,\nu})), \nu = x, y, z. \tag{2}$$

Furthermore, to achieve the objective of distributed consensus under a directed communication topology, we design the following dynamic system to generate the reference position $\bar{p}_{i,d}$ and yaw angle $\psi_{i,d}$ for the ith UAV as

$$\dot{\bar{p}}_{i,d} = k_{i,1} \sum_{j\in\mathcal{N}_i} a_{ij}(\bar{p}_j - \bar{p}_i), \tag{3a}$$

$$\dot{\psi}_{i,d} = k_{i,2} \sum_{j\in\mathcal{N}_i} a_{ij}(\psi_j - \psi_i), \tag{3b}$$

where $k_{i,1}$ and $k_{i,2}$ are positive constants.

In the sequel, we design the distributed control inputs T_i and τ_i for the ith, $i = 1, \ldots, n$, UAV so that its transformed position $\bar{p}_i$ and yaw angle ψ_i can converge to the reference position $\bar{p}_{i,d}$ and yaw angle $\psi_{i,d}$, respectively. As the UAV modeled by (1) possesses the higher-order nonlinear dynamics with mismatched conditions, the control design will be proceeded by adopting a backstepping-like methodology.

Step 1 (Position Control Loop): In this step, we design the thrust T_i, the virtual roll $\phi_{i,d}$, and the virtual pitch $\theta_{i,d}$ such that the transformed position $\bar{p}_i$ can track $\bar{p}_{i,d}$. To begin the development, we define the position tracking error as $e_{i,p} = [e_{i,x}, e_{i,y}, e_{i,z}]^T = \bar{p}_i - \bar{p}_{i,d}$. By (2), the first and second derivatives of $\bar{\nu}_i$, $\nu = x, y, z$, can be computed as

$$\dot{\bar{\nu}}_i = \frac{(-L_\nu + U_\nu)(\dot{\nu}_i - \dot{\triangle}_{i,\nu})}{(-L_\nu + (\nu_i - \triangle_{i,\nu}))(U_\nu - (\nu_i - \triangle_{i,\nu}))},$$

$$\begin{aligned} \ddot{\bar{\nu}}_i &= \tfrac{(L_\nu - U_\nu)(L_\nu + U_\nu - 2(\nu_i - \triangle_{i,\nu}))}{(L_\nu - (\nu_i - \triangle_{i,\nu}))^2 (U_\nu - (\nu_i - \triangle_{i,\nu}))^2}(\dot{\nu}_i - \dot{\triangle}_{i,\nu})^2 \\ &\quad + \tfrac{(-L_\nu + U_\nu)(\ddot{\nu}_i - \ddot{\triangle}_{i,\nu})}{(-L_\nu + (\nu_i - \triangle_{i,\nu}))(U_\nu - (\nu_i - \triangle_{i,\nu}))}. \end{aligned}$$

Thus, we can obtain the following relationship

$$\ddot{\bar{p}}_i = [\ddot{\bar{x}}_i, \ddot{\bar{y}}_i, \ddot{\bar{z}}_i]^T = C_i \ddot{p}_i + \eta_i, \tag{4}$$

[1]Throughout the following development, we denote with $\mathbf{1}_m$ and $\mathbf{0}_m$, respectively, the $m-$vector of all ones and all zeros, and we let I_m denote the $m-$dimensional identity matrix.

where $C_i = \mathrm{diag}\{c_{i,x}, c_{i,y}, c_{i,z}\}$ and $\eta_i = [\eta_{i,x}, \eta_{i,y}, \eta_{i,z}]^T$ with

$$\begin{aligned} c_{i,\nu} &= \frac{-L_\nu+U_\nu}{(-L_\nu+(\nu_i-\triangle_{i,\nu}))(U_\nu-(\nu_i-\triangle_{i,\nu}))}, \\ \eta_{i,\nu} &= \frac{(L_\nu-U_\nu)(L_\nu+U_\nu-2(\nu_i-\triangle_{i,\nu}))}{(L_\nu-(\nu_i-\triangle_{i,\nu}))^2(U_\nu-(\nu_i-\triangle_{i,\nu}))^2}(\dot{\nu}_i-\dot{\triangle}_{i,\nu})^2 \\ &\quad -\frac{(-L_\nu+U_\nu)\ddot{\triangle}_{i,\nu}}{(-L_\nu+(\nu_i-\triangle_{i,\nu}))(U_\nu-(\nu_i-\triangle_{i,\nu}))}, \nu = x, y, z. \end{aligned}$$

Substituting (1) into (4), we have that $\ddot{e}_{i,p} = C_i(\bar{R}_i T_i/m_i - \mathrm{g}\bar{e}_3) + \eta_i - \ddot{\bar{p}}_{i,d}$, where $\ddot{\bar{p}}_{i,d} = k_{i,1}\sum_{j\in\mathcal{N}_i} a_{ij}(\dot{\bar{p}}_j - \dot{\bar{p}}_i)$. We define the sliding mode error as $s_{i,p} = \lambda_{i,p}e_{i,p} + \dot{e}_{i,p}$, where $\lambda_{i,p}$ is a positive constant. The derivative of $s_{i,p}$ satisfies

$$\begin{aligned} \dot{s}_{i,p} &= \lambda_{i,p}\dot{e}_{i,p} + \ddot{e}_{i,p} \\ &= \lambda_{i,p}\dot{e}_{i,p} + C_i(\tfrac{1}{m_i}\bar{R}_i T_i - \mathrm{g}\bar{e}_3) + \eta_i - \ddot{\bar{p}}_{i,d}. \end{aligned} \tag{5}$$

Based on (5), we design the virtual position tracking controller $\alpha_i = [\alpha_{i,x}, \alpha_{i,y}, \alpha_{i,z}]^T$ shown below

$$\alpha_i = \frac{1}{m_i}\bar{R}_{i,d}T_i = \mathrm{g}\bar{e}_3 + C_i^{-1}(\ddot{\bar{p}}_{i,d} - \eta_i - q_{i,p}s_{i,p} - \lambda_{i,p}\dot{e}_{i,p}), \tag{6}$$

where $\bar{R}_{i,d} = [\cos\phi_{i,d}\sin\theta_{i,d}\cos\psi_{i,d} + \sin\phi_{i,d}\sin\psi_{i,d}, \cos\phi_{i,d}\sin\theta_{i,d}\sin\psi_{i,d} - \sin\phi_{i,d}\cos\psi_{i,d}, \cos\phi_{i,d}\cos\theta_{i,d}]^T$, and $q_{i,p}$ denotes a positive constant.

Since the virtual position tracking controller α_i has been defined in (6), noting that $\|\bar{R}_{i,d}(t)\| = 1$, we select the thrust T_i as

$$T_i(t) = m_i\|\alpha_i(t)\|. \tag{7}$$

Considering the developed virtual position tracking controller α_i in (6) and $\psi_{i,d}$ in (3b), we design the virtual roll $\phi_{i,d}$ and virtual pitch $\theta_{i,d}$ as follows

$$\begin{aligned} \phi_{i,d} &= \arcsin\left(\frac{\alpha_{i,x}\sin\psi_{i,d} - \alpha_{i,y}\cos\psi_{i,d}}{\sqrt{\alpha_{i,x}^2+\alpha_{i,y}^2+\alpha_{i,z}^2}}\right), \\ \theta_{i,d} &= \arctan\left(\frac{\alpha_{i,x}\cos\psi_{i,d} + \alpha_{i,y}\sin\psi_{i,d}}{\alpha_{i,z}}\right). \end{aligned} \tag{8}$$

Step 2 (Attitude Control Loop): In this step, we intend to present the control input τ_i for the ith UAV such that the attitude γ_i can track $\gamma_{i,d}$, where $\gamma_{i,d} = [\phi_{i,d}, \theta_{i,d}, \psi_{i,d}]^T$. Defining the attitude tracking error $e_{i,\gamma}$ as $e_{i,\gamma} = [e_{i,\phi}, e_{i,\theta}, e_{i,\psi}]^T = \gamma_i - \gamma_{i,d}$ and the sliding mode error as $s_{i,\gamma} = \lambda_{i,\gamma}e_{i,\gamma} + \dot{e}_{i,\gamma}$ with $\lambda_{i,\gamma}$ being a positive constant, we get

$$\begin{aligned} \dot{s}_{i,\gamma} &= \lambda_{i,\gamma}\dot{e}_{i,\gamma} + \ddot{e}_{i,\gamma} \\ &= \lambda_{i,\gamma}\dot{e}_{i,\gamma} + f_i + g_i\tau_i - \ddot{\gamma}_{i,d}. \end{aligned} \tag{9}$$

The control input τ_i is proposed as

$$\tau_i = g_i^{-1}\left(\ddot{\gamma}_{i,d} - (\frac{9T_i^2\bar{c}_i^2}{2\lambda_{i,\gamma}^2 q_{i,p}m_i^2} + q_{i,\gamma})s_{i,\gamma} - \lambda_{i,\gamma}\dot{e}_i - f_i\right), \tag{10}$$

where $\bar{c}_i = \max\{c_{i,x}, c_{i,y}, c_{i,z}\}$, and $q_{i,\gamma}$ is a positive constant controller gain.

IV. Main result and proof

Now, we have completed the distributed control protocol design procedure for the multiple UAVs in a constrained environment. The overall control structure is exhibited in Fig. 1. The main result of this work is established in the following theorem.

Theorem 1: Consider a system consisting of n UAVs (1) and suppose that Assumption 1 holds. If the directed graph $\mathcal{G}$ associated with the communication topology among these UAVs contains a spanning tree, the proposed distributed control algorithms (7) and (10) ensure that (i) $\lim_{t\to\infty}[(p_i(t) - \triangle_i(t)) - (p_j(t) - \triangle_j(t))] = \mathbf{0}_3$ and $\lim_{t\to\infty}(\psi_i(t) - \psi_j(t)) = 0$, and (ii) $L_x < x_m(t) - \triangle_{m,x}(t) < U_x$, $L_y < y_m(t) - \triangle_{m,y}(t) < U_y$, and $L_z < z_m(t) - \triangle_{m,z}(t) < U_z$ for all $t \geq 0$, where $i, j, m = 1, \ldots, n$ and $i \neq j$.

Proof: To prove Theorem 1, we define the nonempty and open set $\Omega = \{\xi \in R^{9n} | L_\nu < \beta_{i,\nu} < U_\nu, \nu = x, y, z, i = 1, \ldots, n\}$, where $\xi = [\beta^T, s^T]^T$ with $\beta = [\beta_1^T, \ldots, \beta_n^T]^T$, $\beta_i = [\beta_{i,x}, \beta_{i,y}, \beta_{i,z}]^T = p_i - \triangle_i$, $s_i = [s_{i,p}^T, s_{i,\gamma}^T]^T$. Notice from Assumption 1 that $\xi(0) \in \Omega$. Besides, it can be checked that the unique solution ξ exists over the set Ω. Let its maximum interval of existence be $[0, t_f)$ with $t_f \in (0, \infty]$, i.e., $\xi(t) \in \Omega$ for all $t \in [0, t_f)$.

Construct the following Lyapunov function candidate for the ith, $i = 1, \ldots, N$, UAV as $V_i = \frac{1}{2}\|s_{i,p}\|^2 + \frac{1}{2}\|s_{i,\gamma}\|^2$. Taking the time derivative of V_i along (5) and (9) gives

$$\begin{aligned} \dot{V}_i &= s_{i,p}^T(\lambda_{i,p}\dot{e}_{i,p} + C_i(\tfrac{1}{m_i}\bar{R}_i T_i - \mathrm{g}\bar{e}_3) + \eta_i - \ddot{\bar{p}}_{i,d}) \\ &\quad + s_{i,\gamma}^T(\lambda_{i,\gamma}\dot{e}_{i,\gamma} + f_i + g_i\tau_i - \ddot{\gamma}_{i,d}). \end{aligned} \tag{11}$$

Substituting the control inputs (6) and (10) into (11) yields

$$\begin{aligned} \dot{V}_i &= -q_{i,p}\|s_{i,p}\|^2 - (\tfrac{9T_i^2\bar{c}_i^2}{2\lambda_{i,\gamma}^2 q_{i,p}m_i^2} + q_{i,\gamma})\|s_{i,\gamma}\|^2 \\ &\quad + \tfrac{T_i}{m_i}s_{i,p}^T C_i(\bar{R}_i - \bar{R}_{i,d}). \end{aligned} \tag{12}$$

Observing that $T_i s_{i,p}^T C_i(\bar{R}_i - \bar{R}_{i,d})/m_i \leq q_{i,p}\|s_{i,p}\|^2/2 + T_i^2\|C_i(\bar{R}_i - \bar{R}_{i,d})\|^2/(2q_{i,p}m_i^2)$ and $\|C_i(\bar{R}_i - \bar{R}_{i,d})\|^2 \leq 9\bar{c}_i^2\|e_{i,\gamma}\|^2 \leq 9\bar{c}_i^2\|s_{i,\gamma}\|^2/\lambda_{i,\gamma}^2$, we obtain the following expression

$$\dot{V}_i \leq -\frac{q_{i,p}\|s_{i,p}\|^2}{2} - q_{i,\gamma}\|s_{i,\gamma}\|^2 \leq 0. \tag{13}$$

Hence, we can conclude from the definition of V_i that the sliding mode errors $s_{i,p}(t)$ and $s_{i,\gamma}(t)$ are bounded on $[0, t_f)$ and subsequently that the tracking errors $e_{i,p}(t)$ and $e_{i,\gamma}(t)$ are bounded on $[0, t_f)$.

Defining the column vectors $\bar{p}_d = [\bar{p}_{1,d}^T, \ldots, \bar{p}_{n,d}^T]^T$, $\bar{p} = [\bar{p}_1^T, \ldots, \bar{p}_n^T]^T$, and $e_p = [e_{1,p}^T, \ldots, e_{n,p}^T]^T$, we can deduce from (3a) that

$$\dot{\bar{p}}_d = -(\bar{\mathcal{L}}_p \otimes I_3)\bar{p} = -(\bar{\mathcal{L}}_p \otimes I_3)(e_p + \bar{p}_d), \tag{14}$$

where $\bar{\mathcal{L}}_p = \mathrm{diag}\{k_{1,1}, \ldots, k_{n,1}\}\mathcal{L}$, and $\otimes$ is the Kronecker product. The solution of (14) is given by

$$\begin{aligned} \bar{p}_d(t) &= \int_0^t e^{-(\bar{\mathcal{L}}_p\otimes I_3)(t-\sigma)}(-(\bar{\mathcal{L}}_p \otimes I_3)e_p(\sigma))d\sigma \\ &\quad + e^{-(\bar{\mathcal{L}}_p\otimes I_3)t}\bar{p}_d(0). \end{aligned} \tag{15}$$

As the directed graph $\mathcal{G}$ associated with the communication topology of the n UAVs contains a spanning tree, by [15, Lemma 2.10] it can be verified that $\bar{\mathcal{L}}_p$ has exactly one zero eigenvalue and all other eigenvalues have positive real parts. It is noted that the linear time-invariant system $\dot{\delta}(t) = -(\bar{\mathcal{L}}_p \otimes I_3)\delta(t)$ is marginally stable [16, p. 138], thus $e^{-(\bar{\mathcal{L}}_p\otimes I_3)t}\bar{p}_d(0)$ is always bounded. For $i, m =$

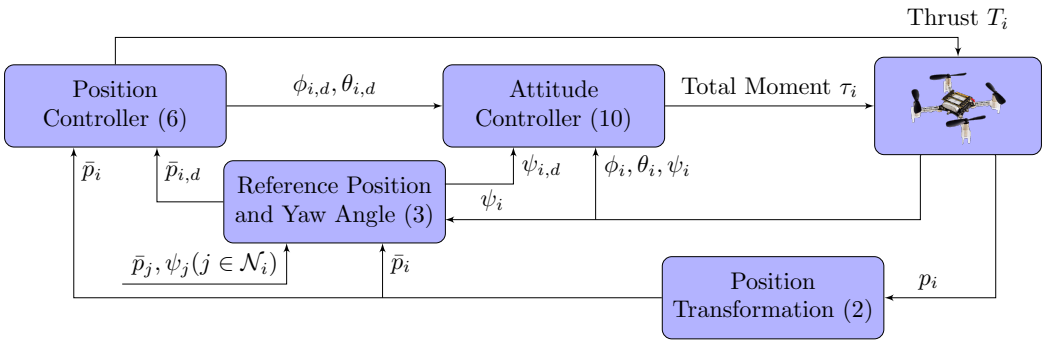

Fig. 1. Structure of the developed distributed consensus control protocol. Given neighbors' information $\bar{p}_j$ and ψ_j ($j \in \mathcal{N}_i$), the position controller and attitude controller generate, respectively, the thrust T_i and the total moment τ_i for the ith UAV to close the loop.

$1, \ldots, n$, let μ_m be the eigenvalues of $-\bar{\mathcal{L}}_p$ and $J = [j_{im}] \in R^{N\times N}$ be the Jordan matrix corresponding to $-\bar{\mathcal{L}}_p$; then we have $j_{mm} = \mu_m$. We assume that $\mu_n = 0$ and μ_m, $m = 1, \ldots, n-1$ have negative real parts. Let $-\bar{\mathcal{L}}_p = D \begin{bmatrix} J_{n-1} & \mathbf{0}_{n-1} \\ \mathbf{0}_{n-1}^T & 0 \end{bmatrix} D^{-1}$, where $J_{n-1} \in R^{(n-1)\times(n-1)}$ is an upper triangular matrix containing all Jordan blocks associated with the eigenvalues μ_1 to μ_{n-1}, and $D \in R^{n\times n}$ is a nonsingular matrix. It is straightforward to see that ω^T is the left eigenvector of $\bar{\mathcal{L}}_p$ related to the eigenvalue 0, with $\omega^T \in R^{1\times n}$ being the last row of the matrix D^{-1}.

Clearly, it can be calculated for $e^{-(\bar{\mathcal{L}}_p \otimes I_3)t}$ that $e^{-(\bar{\mathcal{L}}_p \otimes I_3)t} = (D_{n-1} \otimes I_3)e^{(J_{n-1}\otimes I_3)t}(H_{n-1} \otimes I_3) + \mathbf{1}_n\omega^T \otimes I_3$, where $D_{n-1} = [d_1, \ldots, d_{n-1}]$ and $H_{n-1} = [h_1, \ldots, h_{n-1}]^T$ with d_i being the ith, $i = 1, \ldots, n-1$ column of D, and $h_i^T \in R^{1\times N}$ the ith row of the matrix D^{-1}. Since J_{n-1} is a Hurwitz matrix, the inequality

$$\begin{aligned} 0 &\leq \|\textstyle\int_0^t e^{-(\bar{\mathcal{L}}_p\otimes I_3)(t-\sigma)}(-(\bar{\mathcal{L}}_p \otimes I_3)e_p(\sigma))d\sigma\| \\ &\leq \textstyle\int_0^t \chi_1 e^{-\chi_2(t-\sigma)}\|e_p(\sigma)\|d\sigma \end{aligned} \tag{16}$$

holds for some positive constants χ_1 and χ_2. Based on (16) and the fact that $e_p(t)$ is bounded on $[0, t_f)$, we can conclude that $\int_0^t e^{-(\bar{\mathcal{L}}_p\otimes I_3)(t-\sigma)}(-(\bar{\mathcal{L}}_p \otimes I_3)e_p(\sigma))d\sigma$ is bounded on $[0, t_f)$, which implies that $\bar{p}_d(t)$ is bounded on $[0, t_f)$.

From the boundedness of $e_p(t)$ and $\bar{p}_d(t)$ on $[0, t_f)$, we get that $\bar{p}(t)$ is bounded on $[0, t_f)$. Obviously, it holds that $|\bar{\nu}_i(t)| \leq \nu_i^*$, $\forall t \in [0, t_f)$, $\forall i = 1, \ldots, n$, $\forall \nu = x, y, z$, for some positive constants ν_i^*. Taking the inverse logarithmic function on $\bar{\nu}_i(t)$ leads to

$$L_\nu < \underline{\beta}_{i,\nu} \leq \beta_{i,\nu}(t) \leq \bar{\beta}_{i,\nu} < U_\nu, \forall t \in [0, t_f) \tag{17}$$

where $\underline{\beta}_{i,\nu} = (U_\nu e^{-\nu_i^*} + L_\nu)/(e^{-\nu_i^*} + 1)$ and $\bar{\beta}_{i,\nu} = (U_\nu e^{\nu_i^*} + L_\nu)/(e^{\nu_i^*} + 1)$. We are now ready to show that t_f can be extended to ∞. In this direction, notice by (17) and the boundedness of $s_{i,p}(t)$ and $s_{i,\gamma}(t)$ that $\xi(t) \in \Omega^*$ for all $t \in [0, t_f)$, where Ω^* is a nonempty and compact subset of Ω. Therefore, by Theorem 3.3 in [17], the solution is global, i.e., $t_f = \infty$.

It is straightforward from (13) to see that $\|s_{i,p}\|$ and $\|s_{i,\gamma}\|$ are square integrable. Note that $s_{i,p}$ and $s_{i,\gamma}$ are bounded and from (5) and (9) that $\dot{s}_{i,p}$ and $\dot{s}_{i,\gamma}$ are bounded. Thus, according to Barbalat's lemma, we have that $\lim_{t\to} s_{i,p}(t) = \mathbf{0}_3$ and $\lim_{t\to} s_{i,\gamma}(t) = \mathbf{0}_3$. We can conclude via the definition of $s_{i,p}$ and $s_{i,\gamma}$ that $\lim_{t\to\infty} e_{i,p}(t), \dot{e}_{i,p}(t), e_{i,\gamma}(t), \dot{e}_{i,\gamma}(t) = \mathbf{0}_3$. Therefore, it can be obtained that

$$\lim_{t\to\infty} \int_0^t \chi_1 e^{-\chi_2(t-\sigma)}\|e_p(\sigma)\|d\sigma = 0.$$

By (16), we can further have

$$\lim_{t\to\infty} \int_0^t e^{-(\bar{\mathcal{L}}_p\otimes I_3)(t-\sigma)}(-(\bar{\mathcal{L}}_p \otimes I_3)e_p(\sigma))d\sigma = \mathbf{0}_{3n},$$

which together with the fact that $\lim_{t\to\infty} e^{-(\bar{\mathcal{L}}_p\otimes I_3)t}\bar{p}_d(0) = (\mathbf{1}_n\omega^T \otimes I_3)\bar{p}_d(0)$ gives that $\lim_{t\to\infty} \bar{p}_d(t) = (\mathbf{1}_n\omega^T \otimes I_3)\bar{p}_d(0)$. Furthermore, we can establish via the definition of $e_{i,p}$ that $\lim_{t\to\infty} \bar{p}(t) = \lim_{t\to\infty} e_p(t) + \lim_{t\to\infty} p_d(t) = (\mathbf{1}_n\omega^T \otimes I_3)\bar{p}_d(0)$. Thus, we have that $\lim_{t\to\infty}(\bar{p}_i(t) - \bar{p}_j(t)) = \mathbf{0}_3$, $\forall i, j = 1, \ldots, N$. By the definition of $\bar{p}_i$, over the set Ω^* it holds that

$$\lim_{t\to\infty} \frac{-L_\nu + (\nu_i(t) - \triangle_{i,\nu}(t))}{U_\nu - (\nu_i(t) - \triangle_{i,\nu}(t))} - \frac{-L_\nu + (\nu_j(t) - \triangle_{j,\nu}(t))}{U_\nu - (\nu_j(t) - \triangle_{j,\nu}(t))} = 0, \tag{18}$$

for all $\nu = x, y, z$. Finally, we can obtain that $\lim_{t\to\infty}[(\nu_i(t) - \triangle_{i,\nu}(t)) - (\nu_j(t) - \triangle_{j,\nu}(t))] = 0$ and that $\lim_{t\to\infty}(p_i(t) - \triangle_i(t)) - (p_j(t) - \triangle_j(t)) = \mathbf{0}_3$. Applying the mimicking argument, we can also conclude that $\lim_{t\to\infty}(\psi_i(t) - \psi_j(t)) = 0$. The proof is complete.

V. Simulation and Experimental Implementation

A. Simulation Study

To verify the effectiveness of the proposed control protocol, we performed a simulation study in Coppelia Robotics V-REP. An application example with four quadrotors was considered, in which the dynamics of each quadrotor can be modeled by (1) and its physical

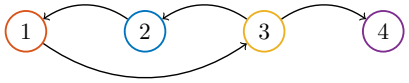

Fig. 2. Communication topology.

parameters are the same as those in [18]. The directed and unweighted graph associated with the communication topology among these four quadrotors is displayed in Fig. 2. The time-varying offsets of the desired distances between the quadrotors and the consensus position were selected as $\triangle_1 = [1.2\cos(t/3), -1.2\sin(t/3), 0]^T$ m, $\triangle_2 = [-1.2\sin(t/3), -1.2\cos(t/3), 0]^T$ m, $\triangle_3 = [-1.2\cos(t/3), 1.2\sin(t/3), 0]^T$ m, and $\triangle_4 = [1.2\sin(t/3), 1.2\cos(t/3), 0]^T$ m. The environmental constraints for the quadrotors were given as $L_x = L_y = -3.5$ m, $U_x = U_y = -3.5$ m, $L_z = 0$ m, and $U_z = 4$ m. The initial conditions for the quadrotors satisfying Assumption 1 were set as $p_1(0) = [0.175, -1.475, 0.2]^T$ m, $p_2(0) = [0.125, 0.85, 0.25]^T$ m, $p_3(0) = [-1.225, 0.35, 0.2]^T$ m, $p_4(0) = [1.625, -0.35, 0.1]^T$ m, $\gamma_1(0) = [0, 0, 0.175]^T$ rad, $\gamma_2(0) = [0, 0, -0.175]^T$ rad, $\gamma_3(0) = [0, 0, 0.262]^T$ rad, and $\gamma_4(0) = [0, 0, -0.262]^T$ rad. Suppose that these quadrotors were hovering at the start, i.e., $\dot{p}_i(0) = \mathbf{0}_3$ m/s and $\dot{\gamma}_i(0) = \mathbf{0}_3$ rad/s for all $i = 1, 2, 3, 4$. The control objective was to design the thrust T_i and the total moment τ_i for each quadrotor so that the positions and yaw angles of all the quadrotors could achieve consensus in the constrained environment. The design parameters of the proposed control protocol were adopted as $k_{i,1} = 1$, $k_{i,2} = 1$, $\lambda_{i,p} = 3$, $\lambda_{i,\gamma} = 10$, $q_{i,p} = 2$, and $q_{i,\gamma} = 0.5$ for all $i = 1, 2, 3, 4$. The initials of $\bar{p}_{i,d}$ and $\psi_{i,d}$ were chosen as $\bar{p}_{1,d}(0) = [-0.4, -0.1, 2.1]^T$, $\bar{p}_{2,d}(0) = [-0.3, 0.2, 2.4]^T$, $\bar{p}_{3,d}(0) = [0.2, -0.3, 2.3]^T$, $\bar{p}_{4,d}(0) = [-0.1, -0.4, 2.2]^T$, and $\psi_{i,d}(0) = 0$.

Simulation results with the proposed distributed consensus control protocol are shown in Figs. 3-6. Specifically, the snapshots of the trajectories of these quadrotors are provided in Fig. 3. The three-dimensional (3D) positions of the quadrotors are presented in Fig. 4, from which we can observe that all quadrotors achieve the consensus and the environmental constraints are not violated at all times. The evolution of the longitudinal and latitudinal relative position errors is depicted in Figs. 5-6.[2] These figures exhibit that the proposed protocol can fulfill the consensus assignment under a directed graph condition and has a satisfactory control performance in a constrained environment.

B. Experimental Study

To demonstrate the real-time performance of the proposed method, an experimental testbed was constructed including the following components: 1) three Crazyflie 2.0 UAVs with two USB radio dongles manufactured by Bitcraze AB; 2) a high-speed motion capture system, the OptiTrack Prime 13 W; and 3) two personal computers (PCs) with Linux OS (Ubuntu 16.04). The motion capture system was employed to track the different pattern of three fluorescent markers mounted on each UAV and then determine the position of each UAV. One PC ran the position control programs of UAV 1 and UAV 2 given by (6), and the other ran the program

[2]It can be seen from Fig. 3 and the supplemental video that the consensus of yaw angles and vertical positions has also been reached. However, the trajectories of them are not presented in this paper due to the limited space.

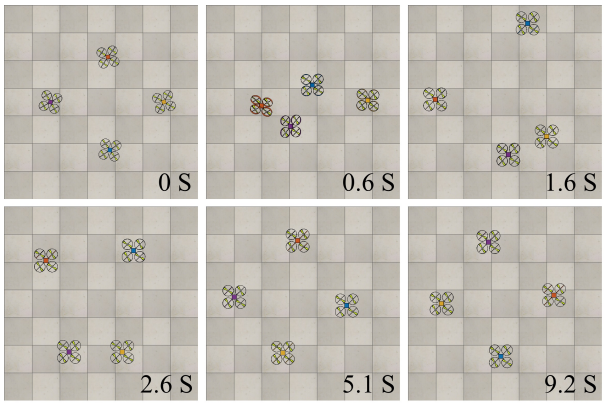

Fig. 3. Consensus of the quadrotors in a constrained environment under the proposed protocol. These frames are taken from a movie that can be found in the supplemental video.

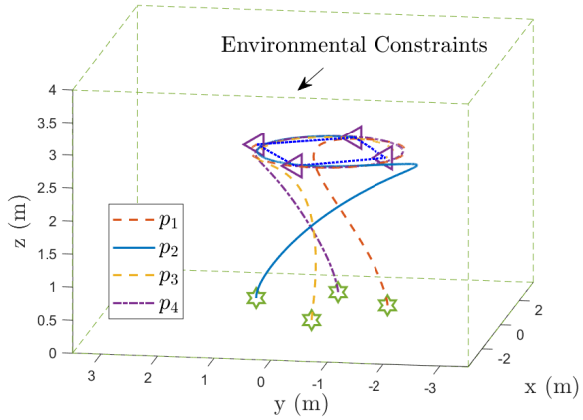

Fig. 4. Simulation results: 3D positions of the quadrotors.

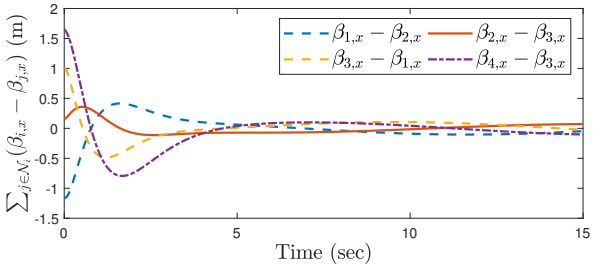

Fig. 5. Simulation results: longitudinal relative errors ($\beta_{i,x} = x_i - \triangle_{i,x}$).

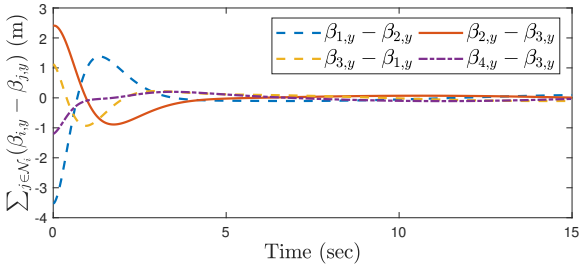

Fig. 6. Simulation results: latitudinal relative errors ($\beta_{i,y} = y_i - \triangle_{i,y}$).

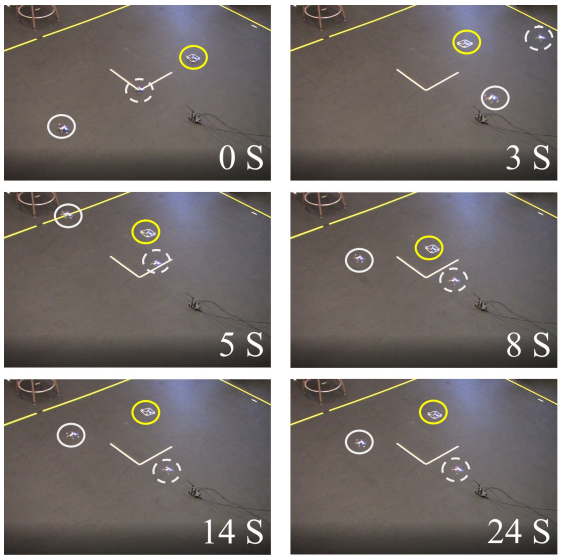

Fig. 7. Consensus of the Crazyflie 2.0 under the proposed protocol. These frames are taken from a movie that can be found in the supplemental video.

of UAV 3, based on which the thrust T_i $(i = 1, 2, 3)$, the desired roll $\phi_{i,d}$ and pitch $\theta_{i,d}$ could be obtained for each UAV. The calculated information was then transmitted from the PCs to the onboard processors of the UAVs via the radio dongles. Though the control programs of UAV 1 and UAV 2 were executed on the same PC, the algorithm was implemented in a distributed way as their positions were not necessarily shared. The communication topology among these three UAVs was the same as that illustrated in Fig. 2. The control objective was to design the control inputs for each UAV such that the positions of all the UAVs could achieve consensus. For simplicity, the constraints were not considered, i.e., $\bar{p}_i$ was defined as $\bar{p}_i = \beta_i = p_i - \triangle_i$ in the experiment. The offsets of the desired distances between the UAVs and the consensus position were constants and were chosen as $\triangle_1 = [0, -0.55, 0]^T$m, $\triangle_2 = [-0.48, 0.28, 0]^T$m, and $\triangle_3 = [0.48, 0.28, 0]^T$m. The design parameters of the proposed control protocol were selected as $k_{i,1} = 0.2$, $\lambda_{i,p} = 20$, $\lambda_{i,\theta} = \lambda_{i,\phi} = 0.5$, $q_{i,p} = 2$, $q_{i,\theta} = q_{i,\phi} = 500$. To guarantee the operation speed, the control of yaw angles was not required and its control parameters were set to zero. For security reasons, the desired vertical position $\bar{z}_{i,d}$ was fixed and selected as 0.4. The reference longitudinal and latitudinal positions $\bar{x}_{i,d}$ and $\bar{y}_{i,d}$ were initialized to $\bar{\nu}_{i,d}(0) = \bar{\nu}_i(0)$, $\nu = x, y$. The reference position $\bar{\nu}_{i,d}$, $\nu = x, y$ of the ith UAV did not update its value to reduce system turbulence and enhance the stability of the closed-loop system as long as the sum of the absolute values of the relative errors is less than 0.1 m, i.e., $\sum_{j\in\mathcal{N}_i} |\bar{\nu}_j - \bar{\nu}_i| \leq 0.1$.

Experimental results with the proposed control protocol are shown in Figs. 7-10. The snapshots of the distributed control of the UAVs are presented in Fig. 7. Fig. 8 exhibits the 3D positions of the UAVs, and the longitudinal and latitudinal relative position errors are, respectively, depicted in Figs. 9-10. From the experimental results, we can conclude that the proposed control algorithm reaches reasonable consensus in a very short time with small residual errors.

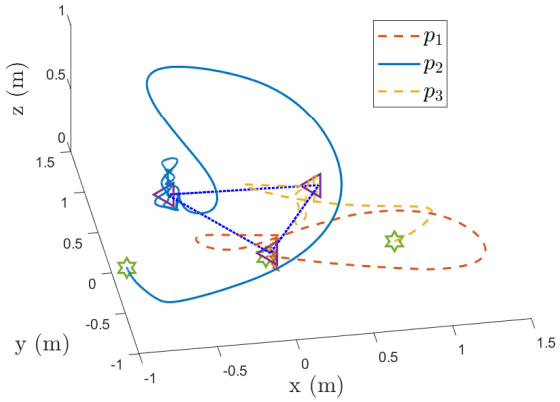

Fig. 8. Experimental results: 3D positions of the UAVs.

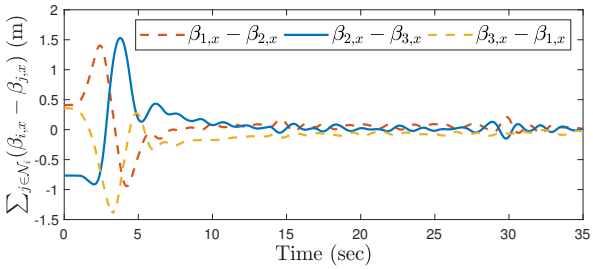

Fig. 9. Experimental results: longitudinal relative errors ($\beta_{i,x} = x_i - \triangle_{i,x}$).

VI. Conclusions

This paper presented our efforts on developing a novel distributed consensus control protocol for multiple UAVs to deal with environmental constraints. The communication topology among the UAVs is assumed to be a general directed graph including a spanning tree. In addition, the input update of each UAV depends only on local state information from its neighborhood set and the constraints, and it does not need any additional centralized information. Further research work is currently underway to extend our methodology to the case of multiple deformable UAVs with dynamically changing interaction topologies.

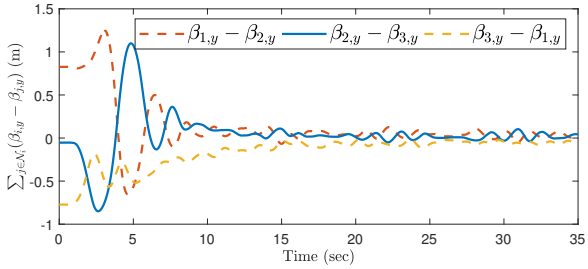

Fig. 10. Experimental results: latitudinal relative errors ($\beta_{i,y} = y_i - \triangle_{i,y}$).

REFERENCES

[1] V. Kumar and N. Michael, "Opportunities and challenges with autonomous micro aerial vehicles," *Int. J. Robot. Res.*, vol. 31, no. 11, pp. 1279–1291, Sep. 2012.

[2] G. Loianno and V. Kumar, "Cooperative transportation using small quadrotors using monocular vision and inertial sensing," *IEEE Robot. Autom. Lett.*, vol. 3, no. 2, pp. 680–687, 2017.

[3] S. Choudhary, L. Carlone, C. Nieto, J. Rogers, H. I. Christensen, and F. Dellaert, "Distributed mapping with privacy and communication constraints: Lightweight algorithms and object-based models," *Int. J. Robot. Res.*, vol. 36, no. 12, pp. 1286–1311, 2017.

[4] Y. Zou, Z. Zhou, X. Dong, and Z. Meng, "Distributed formation control for multiple vertical takeoff and landing UAVs with switching topologies," *IEEE/ASME Trans. Mechatron.*, vol. 23, no. 4, pp. 1750–1761, 2018.

[5] X. Dong, B. Yu, Z. Shi, and Y. Zhong, "Time-varying formation control for unmanned aerial vehicles: Theories and applications," *IEEE Trans. Contr. Syst. Technol.*, vol. 23, no. 1, pp. 340–348, 2014.

[6] B. MacAllister, J. Butzke, A. Kushleyev, H. Pandey, and M. Likhachev, "Path planning for non-circular micro aerial vehicles in constrained environments," in *Proc. IEEE Int. Conf. Robot. Automat. (ICRA)*, 2013, pp. 3933–3940.

[7] J. Chen, T. Liu, and S. Shen, "Online generation of collision-free trajectories for quadrotor flight in unknown cluttered environments," in *Proc. IEEE Int. Conf. Robot. Automat. (ICRA)*, 2016, pp. 1476–1483.

[8] C. Richter, A. Bry, and N. Roy, "Polynomial trajectory planning for aggressive quadrotor flight in dense indoor environments," in *Robotics Research*. Springer, 2016, pp. 649–666.

[9] M. W. Mueller, M. Hehn, and R. D'Andrea, "A computationally efficient motion primitive for quadrocopter trajectory generation," *IEEE Trans. Robot.*, vol. 31, no. 6, pp. 1294–1310, 2015.

[10] S. Tang, J. Thomas, and V. Kumar, "Hold or take optimal plan (hoop): A quadratic programming approach to multi-robot trajectory generation," *Int. J. Robot. Res.*, vol. 37, no. 9, pp. 1062–1084, 2018.

[11] K. P. Tee, S. S. Ge, and E. H. Tay, "Barrier Lyapunov functions for the control of output-constrained nonlinear systems," *Automatica*, vol. 45, no. 4, pp. 918–927, 2009.

[12] W. Meng, Q. Yang, J. Sarangapani, and Y. Sun, "Distributed control of nonlinear multiagent systems with asymptotic consensus," *IEEE Trans. Syst., Man, Cybern., Syst.*, vol. 47, no. 5, pp. 749–757, 2017.

[13] B. Fan, Q. Yang, J. Sarangapani, and Y. Sun, "Output-constrained control of non-affine multi-agent systems with partially unknown control directions," *IEEE Trans. Automat. Contr.*, vol. 64, no. 9, pp. 3936–3942, 2019.

[14] G. Wang, C. Wang, and X. Cai, "Consensus control of output-constrained multiagent systems with unknown control directions under a directed graph," *Int. J. Robust Nonlinear Control*, vol. 30, no. 5, pp. 1802–1818, 2020.

[15] W. Ren and R. W. Beard, *Distributed consensus in multi-vehicle cooperative control*. New York: Springer, 2008.

[16] C.-T. Chen, *Linear system theory and design*. New York: Oxford University Press, 1999.

[17] H. K. Khalil and J. Grizzle, *Nonlinear systems*. Upper Saddle River: Prentice Hall, 2002.

[18] G. Wang, W. Yang, N. Zhao, P. Li, Y. Shen, and C. Wang, "An approximation-free simple control scheme for uncertain quadrotor systems: Theory and validations," in *Proc. IEEE/RSJ Int. Conf. Intell. Robots Syst. (IROS)*, 2019, pp. 3078–3083.